# Transport properties of nuclear matter from anomalous fission yields

K.-H. Schmidt1\*, Ch. Schmitt2,3, A. Heinz4

- <sup>1</sup>Rheinstr. 4, 64390 Erzhausen, Germany.
- <sup>2</sup>Institut Pluridisciplinaire Hubert Curien, CNRS/IN2P3-UDS, 67037 Strasbourg Cedex 2, France.
- <sup>3</sup>Institute of Nuclear Physics Polish Academy fo Sciences, 31-342 Krakow, Poland.
- <sup>4</sup>Department of Physics, Chalmers University of Technology, 41296 Gothenburg, Sweden.

#### Abstract

In nuclear fission, a heavy nucleus splits into two fragments, driven by the Coulomb repulsion between the positively charged protons. The fission process is governed by the potential energy and basic transport properties of nuclear matter like inertial mass and viscosity. While inertia induces features of memory, viscosity attenuates these features by damping. Exploring signatures of memory in fission is crucial for overcoming the current severe lack experimental information on the transport properties of nuclear matter. Based on an analysis of hitherto unexplained anomalies in fission-fragment yields and total kinetic energies, we show that the memory of the conditions near the second barrier in the massasymmetry degree of freedom is preserved until scission. Our results are in severe conflict with the widely used assumption that the role of collective inertia in fission dynamics is negligible. They therefore falsify the validity of approaches disregarding the influence of inertia, in particular the use of the Smoluchowski equation<sup>1</sup> in fission modeling. Concomitantly, our work reveals that the widespread assumption of local statistical equilibrium in all collective degrees of freedom along the fission path, which is the foundation of the scission-point model, is violated.

#### Introduction

The properties and the behaviour of the matter in our environment that we normally experience are determined by the electric forces between the electrons of the atoms and molecules on an energy scale of a few electron Volts (eV). On a scale of about 1 million times higher energies, dynamical processes in and between atomic nuclei like fission and fusion, come into play. They are governed by the nuclear forces, which are complex and not fully understood. In

particular, the transport properties of nuclear matter, especially the nature and the magnitude of nuclear viscosity, are in the focus of intensive research since many years.

When we disregard the influence of gravity that stabilizes neutron stars, dense objects of nuclear matter can only exist in the form of atomic nuclei with up to about 300 nucleons. Larger nuclei are unstable against binary fission due to the repulsion of the constituent protons. Thus, investigations on the transport coefficients of nuclear matter can only be performed by studying large-scale collective motions of nuclei, whereby fission is an excellent example. Mesoscopic systems, such as atomic nuclei, are small enough that quantum-mechanical features – typical for microscopic systems – are important. However, they are large enough that their behaviour can be understood to a certain extent by using macroscopic concepts. These are a multidimensional space of collective degrees of freedom, a thermodynamic behaviour of intrinsic excitations and others. This has decisive consequences for the study of the transport properties of nuclear matter.

The nature and the magnitude of nuclear viscosity are connected with the question, whether nuclei behave like water drops, where collective motions are underdamped, or like honey drops, where collective motions are overdamped. Overdamped systems are in statistical equilibrium of the available states at any moment of a dynamical process. Conversely, underdamped systems may deviate from statistical equilibrium due to inertial forces. They arise from converting part of their available energy to kinetic energy of the

accessible collective degrees of freedom. This means that the presence of memory effects in nuclear collective motions is a clear indication for the influence of inertial forces on nuclear collective motion.

Dissipation is the process that damps the collective motion of a viscous object. It converts part of the kinetic energy of the object into intrinsic excitations in an irreversible process. Dissipation appears in many scenarios. Fission plays a special role for studying nuclear dissipation for several reasons: (I) Due to the long mean-free path of the nucleons, one-body dissipation is the dominant damping mechanism in low-energy fission<sup>a</sup>. Therefore, fission is ideal for testing the widely used wall- and-window formula<sup>2</sup> for one-body dissipation. (ii) Fission at low excitation energies offers the opportunity for studying dissipation under the influence of pairing correlations. (iii) Fission provides manifold experimental signatures for deducing influence of dissipation and for determining its magnitude along the entire fission process. Fission cross sections<sup>3</sup>, the number of neutrons, light charged particles and gamma rays emitted before scission<sup>4</sup>, fluctuations in the fragment properties<sup>3</sup>, and odd-even effects in the fragment yields<sup>5</sup> have been exploited.

On the theoretical side, most existing models of nuclear dissipation are essentially classical in nature. The major conflict is about the magnitude of the wall formula<sup>6</sup>. Blocki et al. <sup>2</sup> claim that their formulation of the one-body dissipation is complete and compatible with quantum mechanics. Concerns were raised by Griffin et al. <sup>7</sup> about additional quantum-mechanical effects and by Pal et al. <sup>8</sup> about incomplete chaoticity. Both are assumed to reduce the estimated dissipation

considerably. Despite the effort invested experimentally, conclusions remain unclear, often inconsistent, if not contradictory <sup>4</sup>.

The driving force of fission is the tendency for reducing the energy that is stored in the Coulomb repulsion between the constituent protons. It is determined by the potential-energy landscape, which is the energy of the fissioning system as function of its shape. Once the fission barrier is passed, the system tends to larger elongations and, finally, to the formation of two independent fragments. The motion towards scission ends up in an almost infinite number of final states in the divided fission fragments. Thus, two fissioning nucleus is an open system. However, the fission process is accompanied by many other processes that change its properties, for example the shape and the inner structure, of the fissioning system. All of them are fed by the released Coulomb energy, and, thus, they are orthogonal to the fission direction <sup>9</sup>. The transport coefficients can be very different depending on the shape of the fissioning nucleus (see Appendix). In this work, we focus on the magnitudes of damping in the elongation and in the mass-asymmetric degree of freedom, respectively. The latter is connected with pear-like shapes of the fissioning nucleus, which result in fragments with different masses.

### **Abnormal fission yields**

In the course of an intense search for relevant experimental information on the transport properties of nuclear matter, we noticed abnormal effects in the fragment yields from the fission of light actinides. An anomaly was already observed in the 1970's in the fission excitation functions of isotopes<sup>10</sup>, 11, 12, 13, 14, 15, 16 thorium attributed to the presence of a third minimum in the fission barrier<sup>17</sup>, <sup>18</sup>, <sup>19</sup>, <sup>20</sup>, <sup>21</sup>, <sup>22</sup>. The abnormal behaviour in the fragment yields has not attracted attention before. The impact of these anomalies on nuclear technology was already pointed out in a dedicated publication<sup>23</sup>. In this work, we stress the importance for deducing crucial information on the transport properties of nuclear matter.

a One-body dissipation, which is realized by the transport of single nucleons (described by the window formula) or by reflections of single nucleons at the nuclear surface (described by the wall formula), is believed to prevail at relatively low energies. This situation is typical in the present context. Two-body dissipation, which is realized by nucleon-nucleon collisions prevails at higher energies.

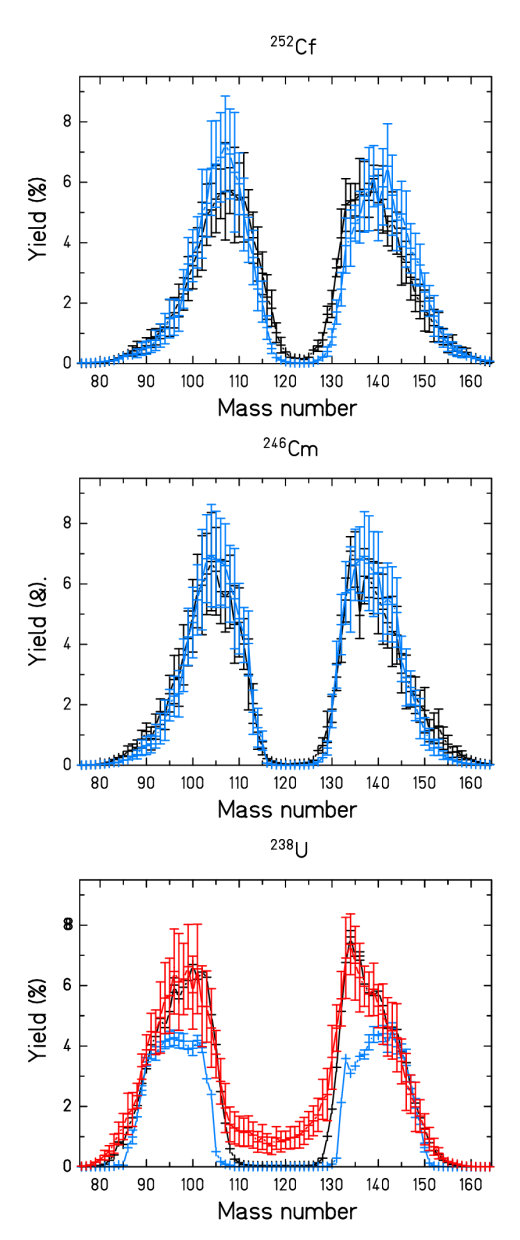


Fig. 1: Illustration of the anomalous shape of the asymmetric peaks in the mass distribution from spontaneous fission of <sup>238</sup>U. The inner parts of the asymmetric peaks are strongly suppressed, in comparison with the data from the fission of <sup>246</sup>Cm and <sup>252</sup>Cf. (Data from ENDF/B-VII<sup>24</sup>)

Blue symbols: spontaneous fission, black symbols: fission induced by neutrons below 2 MeV, red symbols: fission induced by 14-MeV neutrons. The distributions from spontaneous fission and from 14-MeV neutron-induced fission of <sup>238</sup>U were scaled to fit to the yields from fission induced by low-energy neutrons in the range of fragment mass 90. (In some cases, the data from nearby nuclei are shown, due to the lack of available data, see Table 1.)

This is only possible because of the presence of a third barrier. The anomalies and, in particular, their dependence on excitation energy  $E^*$  reflect the magnitude of inertial mass and dissipation by the appearance of memory effects.

Figure 1 shows that in almost all fissioning systems the fragment-mass distributions from fission, thermal-neutron-induced spontaneous fission and 14-MeV-neutron-induced fission are very similar. For higher neutron energies, the main difference is the higher yield near symmetry. This effect is well known due to the enhanced vield of the symmetric fission channel, which is favoured by the macroscopic potential. The observed similarities indicate that the shell effects, which are behind the appearance of the asymmetric components in the mass distribution, are rather insensitive to a variation of the excitation energy of the fissioning system in almost all cases. The theoretically expected reduction of the shell strength with increasing excitation energy does not have an influence on the shape of the asymmetric components. Only the data for spontaneous fission of <sup>238</sup>U differ substantially from the data of neutron-induced fission (thermal to 14-MeV neutrons): The yields of nuclei near the doubly-magic <sup>132</sup>Sn and the corresponding light fragments are strongly reduced. This suggests that there is a particular effect in the dynamics of the fission process in this system appearing at the lowest excitation energy.

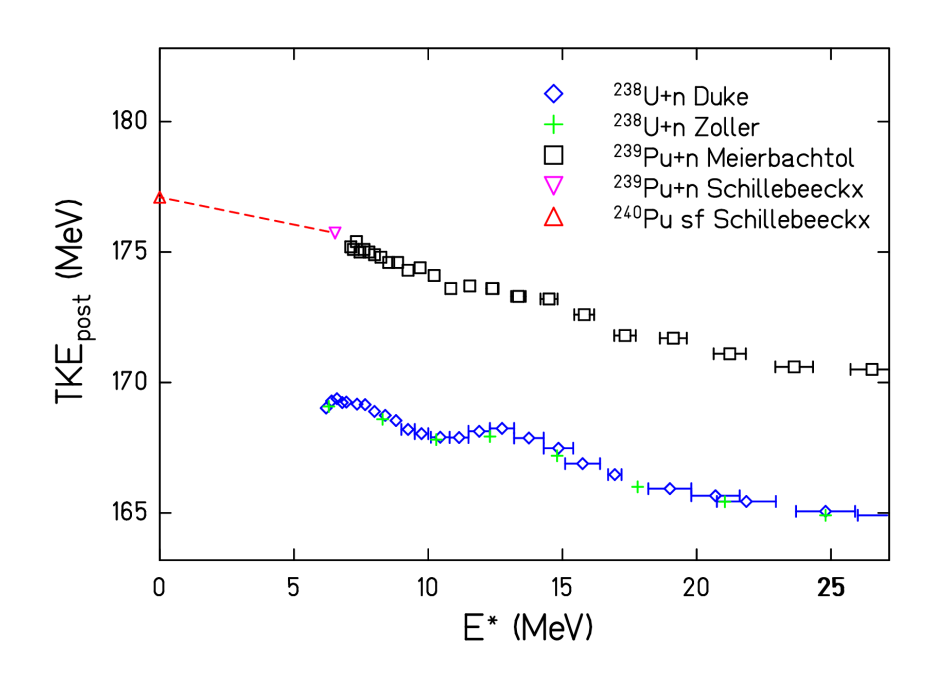
Figure 2 reveals that this suppression effect starts to be seen also in the total kinetic energies in neutron-induced fission of <sup>238</sup>U at the lowest incident-neutron energies. However, there is no suppression seen in the fission of <sup>240</sup>Pu, even from its ground state by spontaneous fission. A similar dependence of the shape of the fragment-yield distribution on the excitation energy was pointed for fission of <sup>233</sup>Pa, induced by protons on <sup>232</sup>Th, see Fig. 3. There, regular oscillations of the peak positions in the mass distributions appear. The peaks of the asymmetric components move towards larger asymmetry, when a sizable part of

the fission events is expected to occur from lighter Pa isotopes at energies close to the fission barrier after the pre-fission emission of one or several neutrons. This brings up the question about the origin of the suppression of the fission yields in the inner wings of the asymmetric peaks in these specific cases. The answer is provided by Fig. 4, which shows the evolution of the potential energy along the fission path for a series of systems.

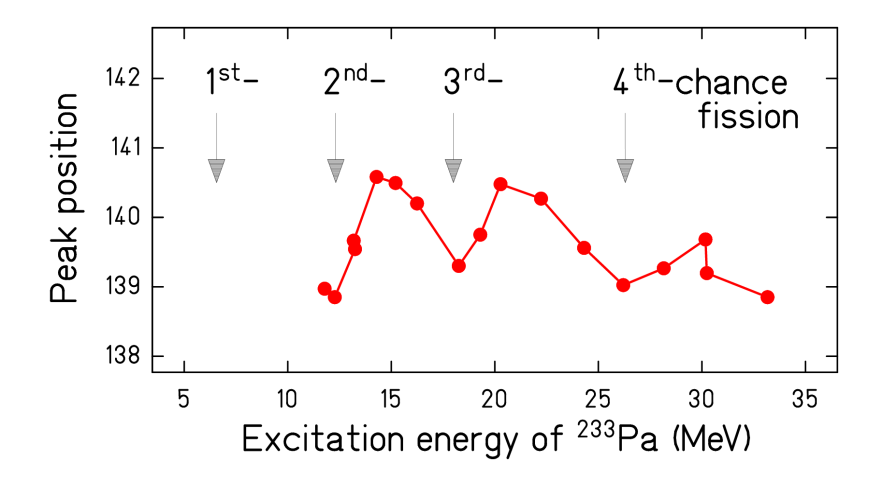
Table 1: List of the fissioning systems used in figure 1.

Nominal system	$^{238}U$	<sup>246</sup> Cm	<sup>250</sup> Cf
Spontaneous fission	<sup>238</sup> U(s,f)	<sup>246</sup> Cm(sf)	<sup>252</sup> Cf(s,f)
Low-energy neutrons	<sup>238</sup> U( $n_{\text{fast}}$ , $f$ ), $E_n \approx 2 \text{ MeV}$	$E_n = \text{thermal}$	$^{249}$ Cf(n <sub>th</sub> ,f), $E_n$ = thermal
High-energy neutrons	$^{238}$ U(n,f), $E_n = 14 \text{ MeV}$	No data available	No data available

Due to the lack of data, in some cases, the values of the nominal systems are not available. Data from nearby systems are shown in these cases. This choice does not have any sizable influence on the conclusions of the present work.



**Fig. 2: Evidence for the suppression effect in TKE.** Measured mean total kinetic energies (TKE) after prompt-neutron emission of the fragments from fission of the compound nuclei  $^{239}$ U and  $^{240}$ Pu from refs.  $^{25}$ ,  $^{26}$ , (neutron-induced and spontaneous fission). The values for spontaneous fission of  $^{240}$ Pu and thermal-neutron-induced fission of  $^{239}$ Pu have been estimated by normalizing the pre-neutron TKE from ref. [4] to the extrapolation of ref. [3] at  $E_n$ =0.586MeV down to thermal energy. The dashed line is drawn to guide the eye. While the TKE from the fission of  $^{240}$ Pu shows a continuous increase with decreasing excitation energy down to spontaneous fission, the TKE from the fission of  $^{239}$ U shows a bending down at the lowest excitation energies. This bending is consistent with the suppression of events with heavy fragments near the doubly magic  $^{132}$ Sn in spontaneous fission of  $^{238}$ U seen in Fig. 1, because these events are known to have the highest TKE values.



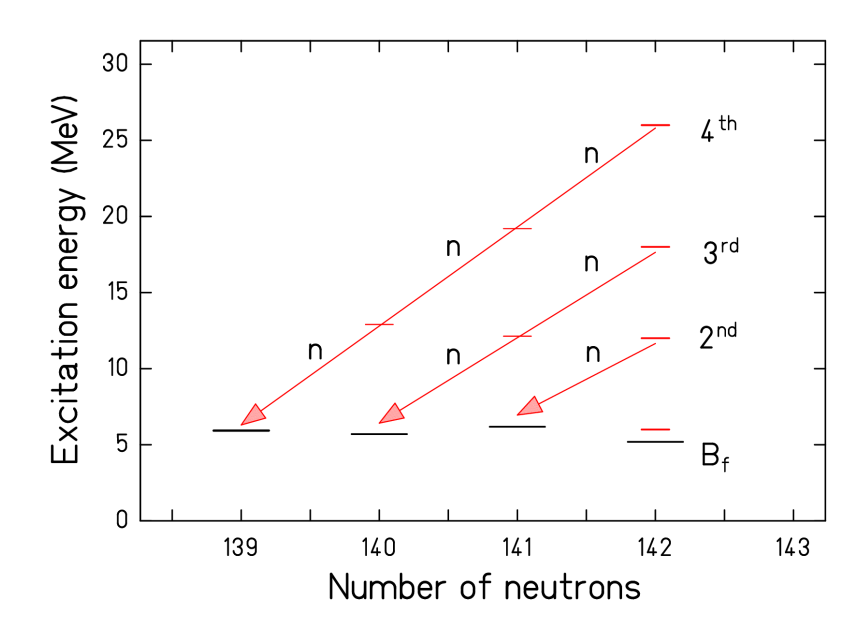


**Fig. 3: Manifestation of the suppression effect in multi-chance fission of** <sup>233</sup>Pa. The upper panel shows the position of the heavy component of the fission-fragment mass distribution from the reaction p + <sup>232</sup>Th as a function of the excitation energy  $E^*$  of the compound nucleus <sup>233</sup>Pa, measured by Berriman et al. <sup>29</sup>. The peak position oscillates and shows minima at  $E^* = 12.5$ , 18 and 26 MeV. The *lower panel* shows the maximum energies (by short horizontal red lines) of the states in <sup>232</sup>Pa (N = 141), <sup>231</sup>Pa (N = 140) and <sup>230</sup>Pa (N = 139), respectively, that are populated by the emission of one to three neutrons, starting from initial states at the above mentioned energies in <sup>233</sup>Pa (also denoted by short horizontal red lines). They are obtained by subtracting the respective neutron separation energies. (The neutron kinetic energies have been disregarded, as they are much smaller.) Apparently, the final states in <sup>232</sup>Pa, <sup>231</sup>Pa and <sup>230</sup>Pa after the emission of one, two and three neutrons, respectively, are close to the heights of the respective fission barriers. Thus, the minima observed in the upper panel correspond to the thresholds of 2<sup>nd</sup>, 3<sup>rd</sup> and 4<sup>th</sup> – chance fission, which are also depicted in the upper panel. The increase of the mean fragment masses above the kink is consistent with the appearance of fission events from low excitation energies at the onset of the next-chance fission with the suppression of compact shapes by the third barrier that we postulate in the present work.

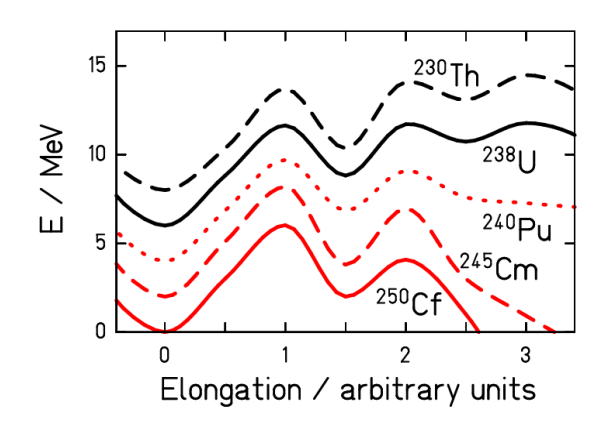


**Fig. 4:** Schematic drawing of the potential energy along the fission path. The curves for Z<98 are displaced by  $\Delta E=(98\text{-}Z)\text{MeV}$  for better visibility. The drawing is based on experimental information about the heights of the first and the second barrier above the ground state (elongation = 0) as well as on the depth of the second minimum, see Table 2. The oscillations that form the multi-humped fission barrier are very similar, while the large-scale (or macroscopic) behaviour that is described by the nuclear liquid-drop model shows a trend from a broad barrier in  $^{230}$ Th to an appreciably narrower one in  $^{250}$ Cf. This trend leads to the appearance of a third barrier with comparable height to the first and the second barrier in the lighter systems.

**Table 2: Potential energy along the fission path.** 

System >	<sup>230</sup> Th ▼	<sup>238</sup> U ▼	<sup>240</sup> Pu ▼	<sup>245</sup> Cm ▼	<sup>250</sup> Cf ▼	Reference ▼
Configura tion ▼						
Ground state	0 MeV	0 MeV	0 MeV	0 MeV	0 MeV	Reference energy
First barrier	5.7 MeV	5.64 MeV	5.7 MeV	6.19 MeV	6.02	GEF
Second minimum	(3.0 MeV)	2.5 MeV	2.5 MeV	1.8 MeV	(1.4 MeV)	Van. 1977 <sup>30</sup>
Second barrier	6.09 MeV	5.71 MeV	5.09 MeV	4.95 MeV	4.08 MeV	GEF
Third barrier	(6.48 MeV)	(5.78 MeV)	(3.27 MeV)	(-1.08 MeV)	(-8.66 MeV)	

The values refer to specific configurations. They are used in Fig. 4. Values in parentheses are estimated by interpolation or extrapolation of empirical trends. Values from GEF<sup>31</sup> are based on the topographic theorem with macroscopic barriers from Thomas-Fermi calculations and empirical ground-state shell effects. They have been validated by measured fission probabilities.

The observed anomaly appears when the system encounters a third barrier with an excitation energy that falls below the third barrier or close to it. The suppressed region in the inner wings of the asymmetric peaks corresponds to very compact configurations with a spherical heavy fragment around the doubly-magic <sup>132</sup>Sn, in agreement with the total kinetic energy signature, see Fig. 2. It is

known that for mass splits in this region the total kinetic energy of the fragments, which is strongly fed by the Coulomb energy in the scission configuration, exploits the Q value almost completely<sup>32</sup>. Therefore, it is expected that the potential at the third barrier is already exceptionally high in this mass range. This makes it rather plausible that the yields are very sensitive

to an eventual variation of the shape of the distortions between the second and the third potential in direction of mass-asymmetric barrier.

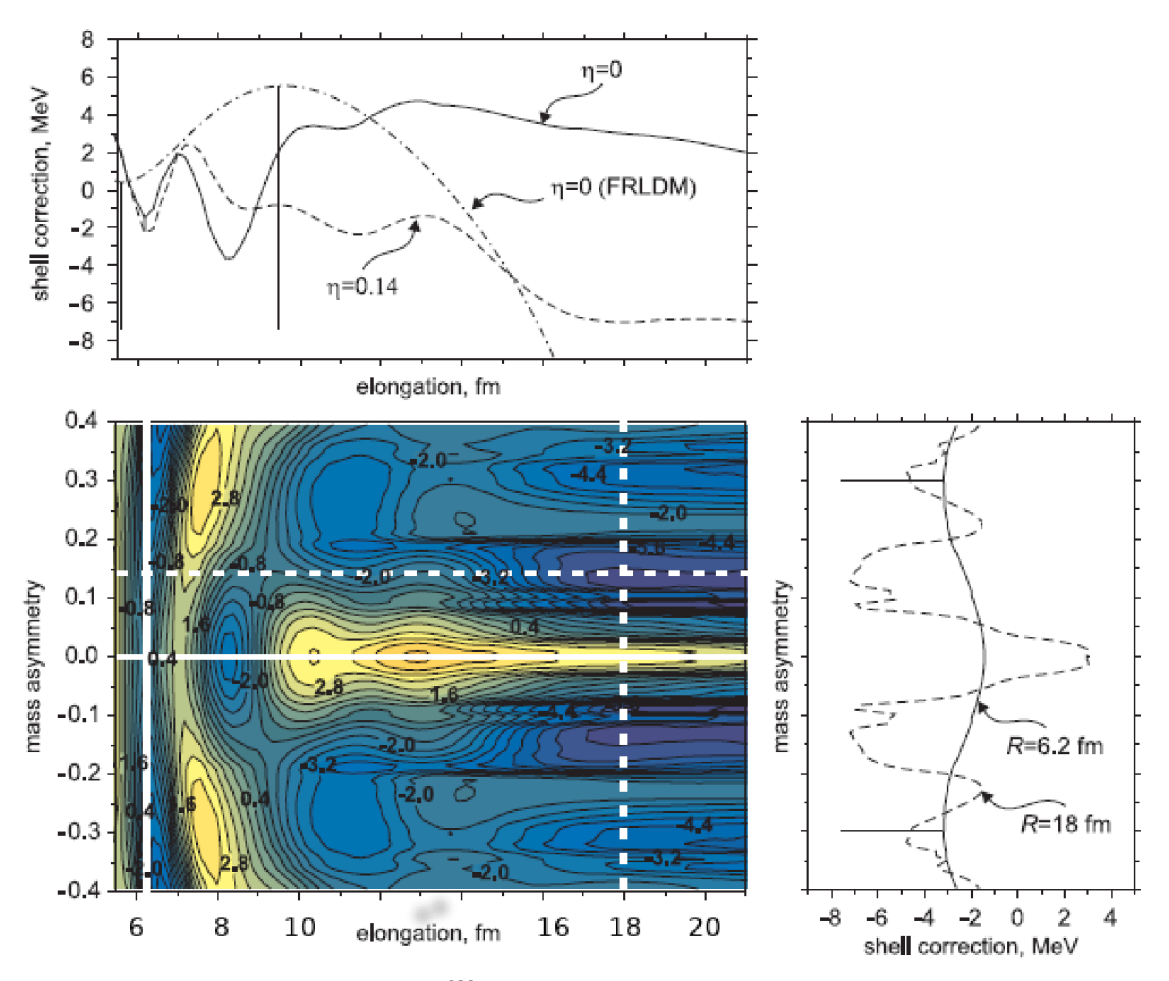


**Fig. 5: Shell-correction energy for the** <sup>238</sup>U nucleus in the coordinates ( $R,\eta$ ). The numbers at the contour lines give the values of the shell correction in MeV. The cuts of the contour plot are made at constant values of the elongation R (6.2 fm and 18 fm) and the mass asymmetry  $\eta$  (0 and 0.14) shown by thick white lines. Types of the lines correspond to those of the cuts. The three humps of the dashed line in the upper graph appear at the first (R = 7 fm), second (R = 9.4 fm) and third barrier (R = 13 fm), respectively, for the mass asymmetry  $\eta = 0.14$ . The dash-dotted curve on the upper graph is the macroscopic potential for symmetric mass split  $\eta = 0$ . (The figure is adapted from ref. [33].)

Figure 5 shows the calculated shell effects of the nucleus  $^{238}$ U from a macroscopic-microscopic model  $^{33}$  on the two-dimensional plane of elongation and mass asymmetric distortions. The tendency for a slight shift of the negative shell correction towards increased mass asymmetry is clearly seen at the elongation of the third barrier (R = 13 fm). This small shift can have substantial impact on the final yields.

The anomalies in the fission yields depicted in Fig. 1, 2 and 3 have a plausible explanation in the suppression of fission events with trajectories passing through compact shapes near scission. We propose the following scenario, which is based on an intuitive understanding of the fission dynamics in the spirit of the multidimensional Langevin dynamics, a well established approach in the field. We refer to the Appendix for a deeper discussion. The suppression effect for splits with heavy fragments around <sup>123</sup>Sn appears, because the

system runs out of energy due to the high potential energy at the third barrier. The system can only proceed to scission by tunneling, and this reduces the probability drastically. At higher initial excitation energy, the system can cross the third barrier without tunneling, even in compact This behaviour configurations. provides information on the memory time of the massasymmetry degree of freedom in comparison with the saddle-to-scission time. If the memory time is short, the system will adapt to the potential at the third barrier, and we see the same narrow mass distribution with the suppression of heavy fragments around <sup>132</sup>Sn also at higher excitation energies. If the memory time is long, the system will retain the mass-asymmetry distortions acquired at or slightly after passing the second barrier.

## Transport properties of nuclear matter

Based on the multiplicity of pre-scission neutrons, light charged particles and gamma rays, Hilscher and Rossner (Ref. 4, page 544) deduced a saddleto-scission time in low-energy fission in the order of 10<sup>-19</sup> to 10<sup>-20</sup> seconds. Although the values determined by other methods do not agree in detail, most of them fall into this rather large time span. Hilscher and Rossner also conclude that this time span indicates that the motion from saddle to scission is overdamped. But, as noted above, this does not mean that the motion in all other degrees of freedom is overdamped, too. The inertial mass mass-asymmetric distortions considerably on the way from saddle to scission: it even tends to diverge close to scission, when the neck diameter shrinks (see Ref. <sup>34</sup>, page 29). This means that the motion along the massasymmetry degree of freedom is considerably slowed down with increasing elongation. According to the yield anomalies discussed above, this leads us to conclude that the memory time of asymmetric shape distortions between the outer barrier and scission is appreciably longer than 10<sup>-20</sup> seconds. An analogy can be made with the explanation for the width of the fissionfragment distribution in the N/Z degree of freedom by a freeze-out of the zero-point motion in the giant isovector dipole resonance before scission due to the strongly increasing inertial mass in this degree of freedom 35. As a consequence of the increasing inertia, the frequency of the resonance decreases so much that the width of the N/Z distribution cannot adjust any more before scission to the adiabatic value that corresponds to the local statistical equilibrium. The memory of the potential energy at the second barrier revealed in our work is caused by the same mechanism in massasymmetric distortions. We note that theoretical estimations for the nucleus <sup>224</sup>Th <sup>36</sup> show a sharp increase of both the inertia and the friction tensor at large mass-asymmetry at elongations slightly beyond the macroscopic fission barrier. Thus, also some influence of the increasing friction may be expected. Though, the magnitude of the inertial mass plays an undeniable role.

The theoretical models that disregard the influence of inertial mass on the fission dynamics, example by using the Smoluchowsky equation<sup>1</sup> or by assuming statistical equilibrium at scission, can reproduce the main features of the measured fission yields, while details are still challenging to describe. The anomaly discussed in this work has been overlooked so far, because it the uncertainties of hardly exceeds Our calculations. work emphasizes significance of this anomaly and its potential to advance the understanding of transport properties of nuclear matter. In addition to the description of the yields themselves, a crucial test of current models would be their ability for reproducing the regular variations of the mean masses in the asymmetric peaks as a function of initial excitation energy, found by Berriman et al. <sup>29</sup>.

A comprehensive quantitative dynamical calculation of fission at low excitation energy, especially when part of the trajectory consists of a tunneling process, challenges current theory. No consistent calculation exists. As a stopgap, Sadhukhan and collaborators<sup>37</sup> used a hybrid model for calculating fragment yields. They

combined the transmission through a barrier by tunneling with classical Langevin dynamics beyond the saddle. Such kind of calculation could help to deduce quantitative conclusions on the transport coefficients of nuclear matter. However, such an undertaking is beyond the scope of this work.

#### **Conclusion**

Our work provides proof for the influence of inertial mass on fission dynamics, based on the sign of memory in the evolution of mass asymmetry in the fission dynamics between the second barrier and scission. This finding contradicts previous opinions about the damping of large-scale collective nuclear motion and contradictions clarifies apparent between conclusions drawn from different investigations. On the empirical side, a perceptible influence of memory has been deduced from a comparison of measured fragment-mass distributions with the result of transport calculations<sup>3</sup> on the basis of the Langevin equations. However, this interpretation is less clear compared to our work, because it is based on the excess of the width parameter with respect to a model calculation. In contrast, on the theoretical side, the result of an advanced microscopic parameter-free calculation using the TDSLDA (time-dependent super-fluid density approximation) has been interpreted as the first microscopic justification for the assumption that the influence of inertia in fission dynamics is irrelevant<sup>38</sup>. Our results are in conflict with this conclusion, which had been raised already by the authors of the first formulation of the one-body dissipation<sup>2</sup>. They also disprove the validity of the Smoluchowski equation in stochastic approaches to fission or equivalent models that disregard the influence of inertia<sup>39</sup>, as well as of statistical scission-point models <sup>40</sup>, <sup>41</sup>, <sup>42</sup>, <sup>43</sup>. In a more general sense, the improved knowledge of the transport coefficients established by our analysis provides new constraints on microscopic models that aim to describe the transport properties of nuclear matter, in particular in large-scale collective motion.

**Author information** Correspondence and requests for materials should be addressed to K.-H. S.

(schmidt-erzhausen@t-online.de).

Acknowledgements We thank Ewald Gold for carefully reading the manuscript. The work was supported by the French-German collaboration between IN2P3-DSM/CEA and GSI, under Agreement No. 19-80. AH is grateful for funding from the Knut and Alice Wallenberg Foundation under KAW 2020.0076.

# **Appendix**

## **Stochastic differential equations**

The terms "potential energy", "inertial mass" and "viscosity" are well known for describing the dynamical processes of massive objects in our environment. The corresponding potential, inertial and friction forces form the decisive ingredients of the Fokker-Plank differential equation<sup>44</sup> or the equivalent Langevin equations <sup>45</sup> b. The inertial mass determines the kinetic energy of an object that moves with a certain velocity. The potential energy is the work that has to be invested for displacing the object against a conservative force. This means that the energy can be retrieved by inverting the displacement. Viscosity is the property of a medium that slows down the velocity of a moving object by dissipating its ordered energy (e.g. the kinetic energy) into a disordered form (e.g. heat) in an irreversible process. Viscosity has an intimate connection with a random force, which is expressed by the Einstein relation. It adds fluctuations to the dvnamics.

# **Modeling of fission dynamics**

The appropriate microscopic approach for the description of a nucleus would be to consider the forces that act between any nucleon with all the others and to solve the appropriate differential equations of motion. This is a tremendously complex task. The problem may be simplified by considering that a nucleus has several properties, which resemble those of a classical drop of a liquid. Some of those are a constant volume, a well defined surface, and a self-consistent adjustment of the shape to the acting forces. In this context, the classical Langevin equations are widely used, and particularly successful, for describing large-scale collective nuclear motions, including fission, although this is not obvious. We

here illuminate the abstractions, assumptions and simplifications, which must be applied for employing such an approach that has been developed for the motion of a point-like object in a viscous medium <sup>2</sup>. The introduction of this relatively simple approach favours an intuitive understanding of the problem tackled in the present work. It will also help to deduce the conditions for Markovian and non-Markovian dynamics<sup>c</sup>.

### Multi-dimensional deformation space

In this approach, the potential energy that depends on the shape of the nucleus is commonly expressed by introducing an abstract multidimensional deformation space. The shape is defined by distortions of a sphere, for example by extending or compressing it in one direction to an ellipsoid. Triaxial shapes are introduced by considering an ellipsoid with three different main axes. Also a pear-like shape can be chosen as additional distortion. In principle, an infinite number of distortions can be defined. A specific, more or less complex, shape corresponds to a point in the multidimensional deformation space. The potential energy at a specific point may be calculated by the microscopic approach mentioned above. For the motion of the point in deformation space, representing a change of the shape, the displacement of at least some nucleons of the nucleus is required. This is connected with a certain kinetic energy. This defines the inertial mass, associated with a certain kind of distortion. However, this definition is not unique. Any modification of the positions of the nucleons that end up in the same shape is possible. Here an additional condition, for example the motion of

b It is not our intention here to introduce the Fockker-Planck equation or the Langevin equations in full detail. For this purpose, we refer to the dedicated literature. Our aim is to introduce the abstract deformation space and the most relevant forces that determine nuclear collective dynamics.

c A non-Markovian process is a random process with the property that the future is dependent on the past. Non-Markovian behaviour means that the information that characterizes the system at a certain moment is not complete. For example, the motion of a massive object depends on the momentum that it has acquired in the past. The system shows non-Markovian features, if only the positional coordinates are considered.

the nucleons with the lowest associated kinetic energy (see ref. <sup>46</sup> about "irrotational" and "rotational flow"), makes the definition of the inertial mass unique. If the motion of the nucleons is accompanied by friction, dissipation arises. The magnitude of inertia and dissipation is given by their respective transport coefficient. The inertial mass and dissipation coefficients may depend on the specific kind of shape distortion, the value of the corresponding distortion as well as on temperature and other parameters. This makes the dynamics of the system in the multi-dimensional deformation space rather complicated.

## Application to nuclear fission

A fissioning nucleus is an open system. That means, it is not bound with respect to the elongation degree of freedom. Instead, the motion towards scission ends up in an almost infinite number of final states in the two fission fragments. However, the fissioning nucleus is bound in any other direction in the multidimensional deformation space. In most directions, this can be represented by a parabolalike potential, modulated by quantum-mechanical shell effects<sup>d</sup>. Strong shell effects favour massasymmetric distortions on the way to scission that lead to fission fragments close to specific numbers of protons and/or neutrons. This is well illustrated bv the double-humped distributions, shown in Fig. 1.

The present work deals with the motion in mass-asymmetric distortions during the directed motion towards scission. The crucial question is, whether the distribution in mass-asymmetric distortion adapts quickly to the shape of the corresponding potential in such a way that the population of states in mass asymmetry matches local equilibrium at any elongation. Our analysis shows that the distribution in mass asymmetry at or close to the second barrier persists up to scission, if there is no tunneling beyond the second barrier.

Consequently, the system behaves non-Markovian-like in the mass-asymmetric direction, if only the deformation values are considered and velocities are disregarded: It has a memory on its dynamic evolution at former times.

d Quantum-mechanical shell effects mean a grouping of the energies of stationary states in a potential pocket.
 There are similarities to standing waves with distinct frequencies of an elastic rope that is fixed on both ends.

- 1 Chandrasekhar, S. Stochastic problems in physics and astronomy. Rev. Mod. Phys. **15**(1), 1 (1943).
- 2 Blocki, J., Borneh, Y., Nix, J. R., Randrup, J., Robel, M., Sierk, A. J. & Swiatecki, W. J. One-body dissipation and super-viscosity of nuclei. *Annals of Physics* **113**, 330 (1978).
- 3 Mazurek, K., Nadtochy, P. N., Ryabov, E. G. & Adeev, G. D. Fission-fragment distributions within dynamical approach. *Eur. Phys. J. A* 53, 79 (2017), Erratum: *Eur. Phys. J. A* 53, 144 (2017).
- 4 Hilscher, D. & Rossner, H. Dynamics of nuclear fission. Ann. Phys. Fr. 17, 471 (1992).
- 5 Ramos, D. et al. Experimental evidence of the effect of nuclear shells on fission dissipation and time. *Phys. Rev. C* **107**, L021601 (2023).
- 6 Bender M. et al. Future of nuclear fission theory. J. Phys. G: Nucl. Part. Phys. 47, 113002 (2020).
- 7 Griffin, J. J. & Dworzecka, M. Quantal one-body dissipation: limitations of the classical wall formula" *Phys. Lett. B* **156**, 139 (1985).
- 8 Pal, S. & Mukhopadhyay, T. Shape dependence of single particle response and the one body limit of damping of multipole vibrations of a cavity. *Phys. Rev. C* **54**, 1333 (1996).
- 9 Nix, J. R. The normal modes of oscillation of a uniformly charged drop about its saddle-point shape *Ann. Phys.* **41**, 52 (1967).
- 10 Back, B. B., Britt, H. C., Garrett, J. D. & Hansen, O. Subbarrier fission resonances in Thisotopes. *Phys. Rev. Lett.* **28**, 1707 (1972).
- 11 Bhandari, B. S. Three-hump fission barrier in <sup>232</sup>Th. *Phys. Rev. C* **19**, 1820 (1979).
- 12 Blons, J. A third minimum in the fission barrier. *Nucl. Phys. A* **502**, 121c (1989).
- 13 Csatlos, M., et al. Resonant tunneling through the triple-humped fission barrier of <sup>236</sup>U. *Phys. Lett. B* **615**, 175 (2005).
- 14 Csige, L. et al. Transmission resonance spectroscopy in the third minimum of <sup>232</sup>Pa. *Phys. Rev. C* **85**, 054306 (2012).
- 15 Csige, L. et al. Exploring the multihumped fission barrier of <sup>238</sup>U via sub-barrier photofission. *Phys. Rev. C* **87** (2013) 044321.
- 16 Oberstedt, A., Oberstedt, S. (2023). The Multi-Humped Fission Barrier.
  In: Tanihata, I., Toki, H., Kajino, T. (eds) Handbook of Nuclear Physics . Springer, Singapore. https://doi.org/10.1007/978-981-15-8818-1 79-2.
- 17 Cwiok, S., Nazarewicz, W., Saladin, J. X., Plociennik, W. & Johnson, A. Hyperdeformation and clustering in the actinide nuclei. *Phys. Lett. B* **322**, 304 (1994).
- 18 Jachimowicz, P., Kowal, M. Skalski, J. Eight-dimensional calculations of the third barrier in <sup>232</sup>Th. *Phys. Rev. C* **87**, 044308 (2013).
- 19 Ichikawa, T., Möller, P., Sierk, A. J., Character and prevalence of third minima in actinide fission barriers. *Phys. Rev. C* **87**, 054326 (2013).
- 20 McDonnell, Nazarewicz, W. & Sheikh, J. Third minima in thorium and uranium isotopes in a self-consistent theory. *Phys. Rev. C* **87**, 054327 (2013).
- 21 Schmitt, C., Pomorski, K., Nerlo-Pomorska, B., Bartel, J. Performance of the Fourier shape parametrization for the fission process. *Phys. Rev. C* **95**, 034612 (2017).
- 22 Okada, K., Wada, T., Capote, R., Carjan, N. Cassini-oval description of the multidimensional potential energy surface for 236U: Role of octupole deformation and calculation of the most probable fission path. *Phys. Rev. C* **107**, 034608 (2023).
- 23 Schmidt, K.-H., Schmitt, Ch., Heinz, A. & Jurado, B. Identifying and overcoming deficiencies of nuclear data on the fission of light actinides by use of the GEF code. *Ann. Nucl. Energy* **208**, 110784 (2024).
- 24 Chadwick, M. B., ENDF/B-VII.1 nuclear data for science and technology: cross sections, covariances, fission product yields and decay data. *Nucl. Data Sheets* **112**, 2287 (2011).
- Duke, D. L., Tovesson, F., Laptev, A. B., Mosby, S., Hambsch, F.-J., Brys, T. & Vidali, M. Fission-fragment properties in U238(n,f) between 1 and 30 MeV. *Phys. Rev.* C **94**, 054604 (2016).
- 26 P. Zöller, PhD thesis, Techn. Hochschule Darmstadt, Germany (1995).
- 27 Meierbachtol, K. et al. Total kinetic energy release in Pu239(n,f) post-neutron emission from 0.5 to 50 MeV incident neutron energy. *Phys. Rev.* C **94**, 034611 (2016).
- 28 Schillebeeckx, P., Wagemans, C., Deruytter, A. J. & Barhelemy, R. Comparative study of the fragments' mass and energy characteristics in the spontaneous fission of 238Pu, 240Pu and 242Pu and in the thermal-neutron-induced fission of 239Pu. *Nucl. Phys.* A **545**, 623 (1992).
- 29 Berriman, A., et al. Energy dependence of p + 232 Th fission mass distributions: Mass-asymmetric standard I and standard II modes, and multichance fission. *Phys. Rev. C* **105**, 064614 (2022).
- 30 Vandenbosch, R. Spontaneously fissioning isomers. Ann. Rev. Nucl. Sc. 27, 1 (1977).
- 31 Schmidt, K.-H., Jurado, B., Amouroux & C., Schmitt, C. General description of fission observables: GEF model code. *Nucl. Data Sheets* **131**, 107 (2016).
- 32 Gönnenwein, F., Börsig, B. Tip model of cold fission Nucl. Phys. A 530, 27 (1991).

- 33 Karpov, A. V., Kelic, A., Schmidt, K.-H. On the topographical properties of fission barriers. J. Phys. G: Nucl. Part. Phys. 35, 035104 (2008).
- 34 Nix, J. R. & Swiatecki, W. J. Studies in the liquid-drop theory of nuclear fission. *Nucl. Phys.* 71, 1 (1965).
- 35 Nifenecker, H. A dynamical treatment of isobaric widths in fission: An example of frozen quantal fluctuations. *J. Physique Lett.* **41**, 47 (1980).
- 36 Adeev, G. D., Karpov, A. V., Nadtochii, P. N. & Vanin, D. V. Multidimensional stochastic approach to the fission dynamics of excited nuclei. *Phys. Part. Nucl.* 36, **378** (2005).
- 37 Sadhukhan, J., Nazarewicz, W. & Schunk, N. Microscopic modeling of mass and charge distributions in the spontaneous fission of <sup>240</sup>Pu. *Phys. Rev. C* **93**, 011304(R) (2016).
- 38 Bulgac, A., Jin, S. & Stetcu, I. Nuclear fission dynamics: past, present, needs, and future. *Front. Phys.* **8**, 63 (2020).
- 39 Randrup, J. & Möller, P. Brownian shape motion on five-dimensional potential-energy surfaces: Nuclear fission-fragment mass distributions. *Phys. Rev. Lett.* **106**, 132503 (2011).
- 40 Wilkins, B. D., Steinberg, E. P. & Chasman, R. R. Scission-point model of nuclear fission based on deformed-shell effects. Phys. Rev. C 14, 1832 (1976).
- 41 Carjan, N., Ivanyuk, F. A. & Oganessian, Yu. Ts. Pre-scission model predictions of fission fragment mass distributions for super-heavy elements. *Nucl. Phys. A* **968**, 453 (2017).
- 42 Pasca, H., Andreev, A. V., Adamian, G. G. & Antonenko, N. V. Simultaneous description of charge, mass, total kinetic energy, and neutron multiplicity distributions in fission of Th and U isotopes. *Phys. Rev. C* **104**, 014604 (2021).
- 43 Lemaitre, J.-F., Goriely, S., Hilaire, S. & Sida, J.-L. Fully microscopic scission-point model to predict fission fragment observables. *Phys. Rev. C* **99**, 034612 (2019).
- 44 Abe, Y., Reinhard, P.-G., Suraud, E. On stochastic approaches of nuclear dynamics. *Phys. Rep.* **275**, 49 (1996).
- 45 Langevin, P. Sur la théorie du mouvement brownien [On the theory of Brownian Motion]. *C. R. Acad. Sci. Paris.* **146**, 530 (1908).
- 46 Nix, J. R., Swiatecki, W. J. Studies in the liquid-drop theory of nuclear fission. *Nucl. Phys.* **71**, 1 (1965).